

## Moving Trend Based Filters Design in Frequency Domain

Jan Tadeusz Duda  
AGH University of Science  
and Technology,  
Al. A. Mickiewicza 30,  
30-059 Krakow, Poland  
Email: jdu@agh.edu.pl

Tomasz Pelech-Pilichowski  
AGH University of Science  
and Technology,  
Al. A. Mickiewicza 30,  
30-059 Krakow, Poland  
Email: tomek@agh.edu.pl

**Abstract**—An original approach to digital moving trend based filters (MTF) design, based on Bode plots analysis is proposed, aimed at seasonal time series decomposition and prediction. A number of polynomials of different range are discussed to be used in the MTF as the LS approximation formula. The Bode plots of the MTF are shown, and the best filter is selected. Results of a seasonal time series decomposition and prediction with the best MTF is presented and compared to the classical MTF calculations (involving the linear LS approximation).

### I. INTRODUCTION

The nonstationary time series filtering with moving trends is the well known approach to a nonparametric long term trend extraction from the series, aimed at further processing of stationary residuals and the series prediction [1], [2]. The classical moving trend filter (MTF) is based on rolling approximation of the series with the least-square (LS) linear approximation in a moving window [1]. The window width affects the extracted trend smoothness and cyclic components separation effectiveness. However typically, it is adjusted by a trial method, to reach the appropriately smooth nonparametric trend. This paper shows that much better smoothing properties and cyclic component extraction may be reached by using in MTF a higher order polynomial approximations and by specification of the required filter properties in frequency domain. Hence, the MTF design is proposed by analysis of Bode plots [4] of a number of the filter variants. The MTFs designed in this way were successfully applied to analysis of hydrogeological data [5] and to financial time series prediction [6]. Smoothing and prediction of a step change and a cyclic signal with the studied MTF was shown to illustrate their properties.

### II. MOVING TREND BASED FILTERS – FORMAL BASIS AND PROPERTIES

Nonstationary time series  $y(t)$  may be viewed as the sum of an aperiodic trend function  $f(t)$ , a cyclic component  $C(t)$  of time period  $T$ , and a higher frequency zero-average noise  $z(t)$  [3], [7]:

$$y(t) = f(t) + C(t) + z(t) \quad (1)$$

The periodic component can be written in the form of the harmonic series [4]:

$$C(t) = \sum_{k=1}^K A_k \sin(\omega_T i_k (t - \tau_k)), \quad \omega_T = \frac{2\pi}{T} \quad (2)$$

where  $i_k, k=1, \dots, K$  denote the set of harmonics indices of the consecutive components  $k=1, \dots, K$  (e.g.  $i_k=1, 2, 10$ ),  $A_k$  – the amplitude of  $i_k$ -th harmonic,  $\tau_k$  is the delay of the  $k$ -th component.

The nonparametric trend  $f(t)$  may be calculated for each time step  $t_n$  by a low-pass digital filter designed in such a way to remove the  $\omega_T$  and higher frequency components from the original series  $y(t)$ . The cyclic component  $C(t)$  can be extracted from the filtering residuals by the Least Square (LS) approximation with the regression model of the form (2), and then, the regression residuals  $z(t)$  may be viewed as a high-frequency stochastic process and treated with ARMA approach [2] (if its homoscedasticity can be assumed) or with GARCH models in case of its heteroscedasticity [3].

One of the techniques recommended to calculate the nonparametric trend  $f(t_n)$  is a rolling approximation of the series  $y(t_n)$  with the LS linear approximation in a window containing  $M$  samples, and then averaging of the approximates  $y_F(i, t_n)$  obtained for each  $t_n$  [1]. It is referred to as moving trend based smoothing/filtering, which may be further used to  $h$ -samples ahead prediction of the series main component  $f(t_n+h)$  by its extrapolation with a  $h$ -samples increment  $\Delta_h f$  averaged with harmonic weights [1]:

$$\begin{aligned} f(t_{n+h}) &= f(t_n) + \Delta_h f, \\ \Delta_h f &= \sum_{i=1}^{n-h} C_i \\ C_i &= (f(t_{i+h}) - f(t_i)) \\ C_0 &= 0, C_i = C_{i-1} + \frac{1}{(n-h)(n-h-i+1)} \end{aligned} \quad (3)$$

Hereby we propose a generalization of the moving trend smoothing algorithm, by employing higher order approximating polynomials, with appropriately designed properties. Let us consider the polynomial of the form (4) in the time interval of  $M$  samples, with the time counted from  $-M+1$  to 0:

$$y_F(t_i) \stackrel{def}{=} b_0 + b_1 t_i + b_2 t_i^2 + b_3 t_i^3 + b_4 t_i^4, \quad (4)$$

$$t_i = \{-M+1, \dots, -1, 0\}$$

The derivatives of  $y_{F0}$  at the interval end ( $t_i=0$ ) can be easily shaped by fixing selected coefficients  $b_k$  at zero values, which implies different profiles of the LS approximates  $y_{F_s}$ , as shown in figure 1.

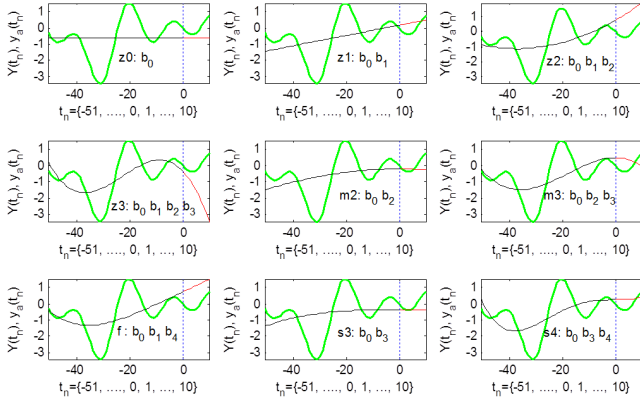


Fig 1. Properties of the approximating polynomials (4) considered to be used in the moving trend based filters; filter codes z0, z1, ..., s3, s4 used in sequel and corresponding nonzero coefficients are listed; vertical dotted line shows the interval end; shadow line:

$$y(t_n) = \sin(0.5\omega_r t_n) - \sin(\omega_r t_n) + \sin(2\omega_r t_n) - \sin(3\omega_r t_n), T=M=52$$

In the moving trend algorithms the series splits into three sections. The first (starting  $s$ ) section begins at the first (oldest) sample and finishes with the  $(M-1)$ -th one, the filtering window width enlarges from  $M$  to  $2M-2$ , and the number  $L_n$  of the approximates  $y_F(i, t_n)$  to be averaged increases from 1 to the  $M-1$ . The second (central  $c$ ) section ranges from the  $M$ -th to  $n-M+1$  samples, the filtering window width is  $2M-1$  (constant), and the number of approximates is  $M$ . The third (final  $f$ ) section contains the samples from  $n-M+2$  to  $n$  (the newest one), the window width reduces from  $2M-2$  to  $M$ , and the number of approximates  $y_F(i, t_n)$  to be averaged decreases from  $M-1$  to 1.

The calculations in the sections  $\{s, c, f\}$  may be expressed in the FIR filtering form [3], [5]:

for  $i = 1, \dots, M-1$ :

$$f(t_i) = \sum_{k=1}^{i+M-1} g_s(i, k) \cdot y(t_{i+M-k})$$

$$= \sum_{k=1}^n G_s(k, i) \cdot y(t_{n-k+1}), \quad (5)$$

$$G_s(k, i) \stackrel{def}{=} [g_s(i, k), 0_{(n-i-M+1)}]^T,$$

for  $i = M, \dots, n-M+1$ :

$$f(t_i) = \sum_{k=1}^{2M-1} g_c(k) \cdot y(t_{i+M-k})$$

$$= \sum_{k=1}^n G_c(k, i) \cdot y(t_{n-k+1}), \quad (6)$$

$$G_c(k, i) \stackrel{def}{=} [0_{(i-M+1)}, g_c, 0_{(n-i-M)}]^T,$$

and for the final section,  $i = n-M+2, \dots, n$ ;

$$j \stackrel{def}{=} i - n + M - 1 = 1, \dots, M - 1 :$$

$$f(t_i) = \sum_{k=1}^{2M-j-1} g_f(j, k) \cdot y(t_{i+M-j-k})$$

$$= \sum_{k=1}^n G_f(k, i) \cdot y(t_{n-k+1}), \quad (7)$$

$$G_f(k, i) \stackrel{def}{=} [0_{(i-M)}, g_f(j, k)]^T$$

where  $g_s, g_c, g_f$  denote the impulse response vectors of filters in the sections  $s, c, f$ , written also as the columns  $G_s, G_c$  and  $G_f$  of the unified smoothing filter matrix  $G_{nx(n-1)}$ , and the proper filter vector  $G(k, n)$ .

Similarly, the prediction formula (3) may be written in the following convolution form:

$$f(t_{n+h}) = \sum_{k=1}^n P_h(k) \cdot y(t_{n-k+1}),$$

$$P_h(k) \stackrel{def}{=} \quad (8)$$

$$G_f(k, M-1) + \sum_{i=1}^{n-h} C_i \cdot (G(k, i+h) - G(k, i)),$$

$$G \stackrel{def}{=} [G_s, G_c, G_f]$$

Notice that  $P_h$  are strongly affected by properties of the proper (the worst) filter  $G_f(k, M-1) = G(k, n)$ .

By making the Fourier Transform of the filters  $g_s, g_c, g_f$  and  $P_h$  involving different approximating polynomial types  $\{z0 \dots s4\}$  with different  $M$  (see fig. 1), one may examine their properties in frequency domain, and select a filtering variant (type,  $M$ ) suitable for smoothing and/or prediction demands, usually related to  $\omega_r$  viewed as the cut-off frequency of the designed low-pass filters. The Bode plots of the examined filters are shown in figures 2-6. We have stated that the approximation window width  $M$  affects directly  $g_s, g_f$  and  $P_h$  delays, but it is of almost no effect on a shape of all the filters gain. Hence  $M$  may be taken as the lowest value producing gains close to 1 for  $\omega < \omega_r$ , near zero for  $\omega = \omega_r$  and close to 0 for  $\omega > \omega_r$ .

Figure 2 shows the central smoothing filters are much better than 1st order recursive ones.

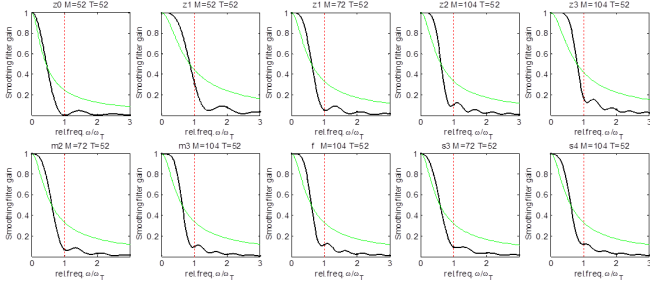


Fig 2. Gain diagrams (vs.  $\omega/\omega_T$ ) for the best smoothing filter (central section); vertical point lines show  $\omega_T$ , shadow solid lines – gain diagram for the 1st order recursive filter of the same half-gain frequency.

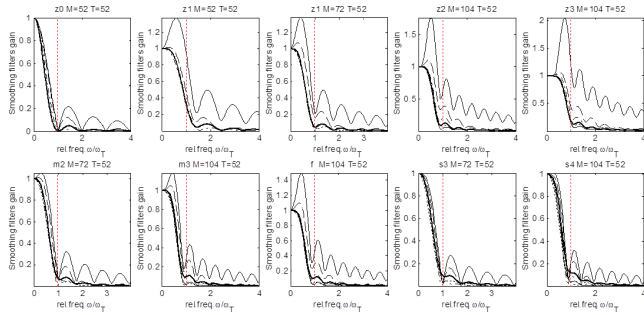


Fig 3. Gain diagrams (vs.  $\omega/\omega_T$ ) for the smoothing filters: central section - bold lines  $h < -M$ , the final section for  $h=0$  solid lines (proper filter),  $h=-20$  dotted lines,  $h=-40$  point-dotted lines.

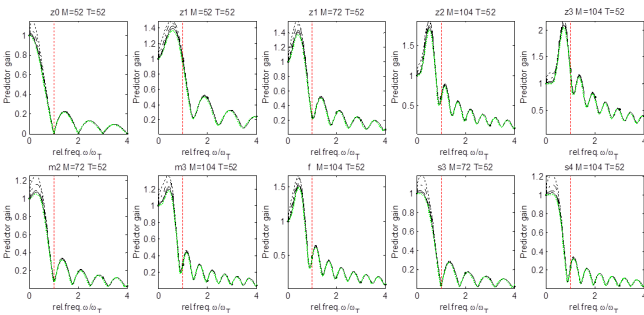


Fig 4. Gain diagrams for the moving trend based predictors: shadow bold line – final filter  $h=0$ ;  $h=5$  solid lines,  $h=10$  dotted lines,  $h=26$  point-dotted lines,  $h=T=52$  point lines.

Gain properties of all the smoothing filters in the central section (fig. 2) are similar. When assuming  $M=1.38 \cdot T=72$ , the classical filter z1 seems to be the best due to the pass-band and attenuation band properties as well as cut-off frequency gain, although z3 pass-band and attenuation of z0 look better. However a view on figures 3 and 4 gives evidence that only z0, s3 and s4 might be accepted from the perspective of final section smoothing (fig. 3) and prediction (fig. 4) properties. In particular, very bad pass and attenuation properties (excessive gain) of the classical filter z1 are clearly seen. Having in mind numerical problems (ill-conditioning) which can be met in s4 for larger  $M$ , one may take that the filter s3 with  $M=72$  ( $1.38T$ ) is the best choice (its pass-band is noticeably better than that of z0). The same conclusion may be drawn on a basis of delay properties shown in figures 5

and 6. In the pass-band a close to uniform and small delay is required (minimum delay distortion of the trend). It is satisfied only by z0 filters, but s4 delay distortion is acceptable and significantly lower than for the classical filter z1. The delay of predictors is larger than that of the final filter ( $h=0$ ) by prediction horizon (see fig. 7). It means that the MTF prediction (eq. 3) does not differ essentially from Zero Order Hold of the  $f(t_n)$ .

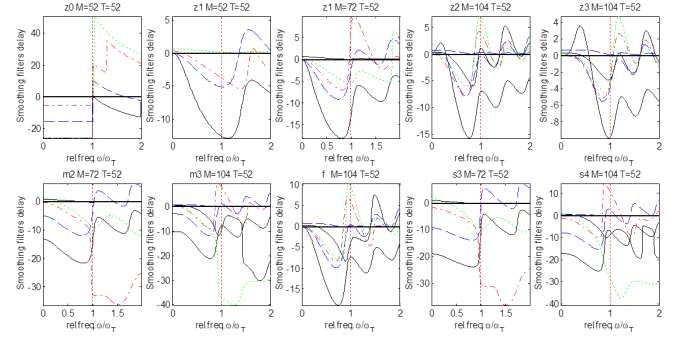


Fig 5. Delay of the final section smoothing filters:  $h=0$  solid lines,  $h=-20$  dotted lines,  $h=-40$  point-dotted lines,  $h=-60$  point lines,  $h=-70$  solid lines close to the zero-delay, bold-line 0 delay of central section filter.

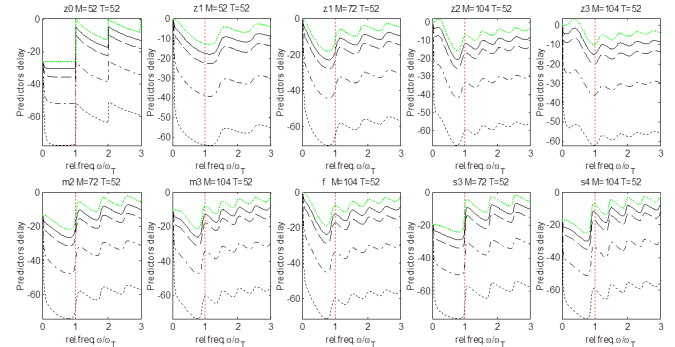


Fig 6. Predictors delay:  $h=0$  shadow point lines,  $h=5$  solid lined,  $h=10$  dotted lines,  $h=26$  point-dotted lines,  $h=T=52$  point lines.

The frequency properties presented above are visible in time domain responses – see figures 8, 9. Step change distortions shown in figure 8 are the larger, the greater irregularities of the pass-band gain and delay.

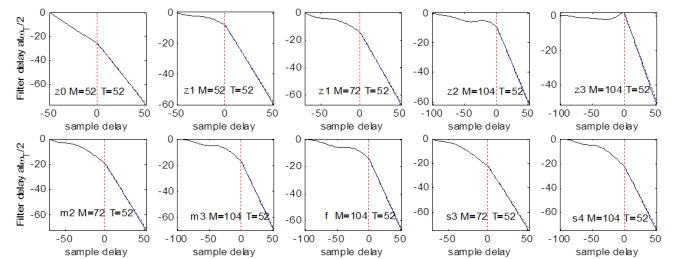


Fig 7. Delay of smoothing filters and predictors for  $\omega_T/2$  versus the sample delay.

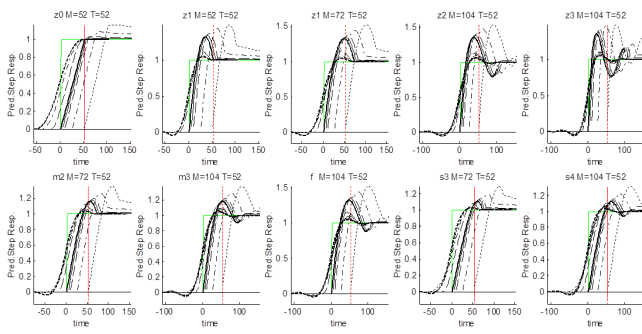


Fig 8. Signal step-wise change smoothing and prediction: shadow bold line – signal; bold dotted line – central segment filter response ( $h < -M$ ); dotted point line smoothing with  $h=40$ ,  $h=-20$  dotted line; bold line final filter response ( $h=0$ ); prediction with  $h=5$  solid lines,  $h=10$  dotted lines,  $h=26$  point-dotted lines,  $h=52$  point lines.

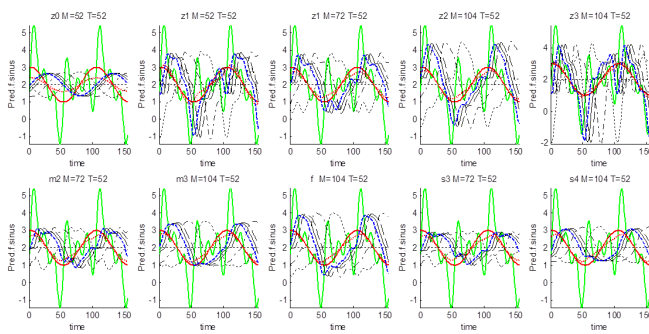


Fig 9. Periodic signal processing with the studied filters: shadow bold line – the signal  $y(t_n)$  (see fig. 1); bold line – the main harmonic of  $y$ ,  $\omega = 0.5\omega_r$  (to be extracted), bold point lines – the main harmonic reconstruction by the central filter response ( $h=-M$ ), the main harmonic reconstruction with the final filter – bold dotted lines, and prediction with  $h=5$  solid lines,  $h=10$  dotted lines,  $h=26$  point-dotted lines,  $h=52$  point lines.

Figure 9 illustrates effects of filtering and prediction of a periodic signal (used also as the example in fig. 1). The harmonic of  $\omega = \omega_r/2$  has to be extracted (reconstructed), but the signal contains strong components in the filters attenuation band. Hence the attenuation gain profile is of significant effect on the extracted signal shape. The best reconstruction is reached with z0 filters. The classical (z2) filters produce highly distorted responses, both in smoothing and prediction cases, while s3 and s4 yield acceptable results. All predictions are similar in shape to the proper filter response ( $h=0$ ) and additionally delayed by the prediction horizon – see fig. 7 (i.e. they do not differ noticeably from ZOH predictions).

The extracted signal distortion in the starting and final sections is significant, hence separation of the filtering residuals into periodic  $C(t)$  and stochastic  $z(t)$  components, by fitting the regression model (2), should be performed with the central section data only. Then the periodic component  $C(t)$  should be extrapolated on the full data interval and subtracted from the filtering residuals to get  $z(t)$ .

### III. CONCLUSION

The classical moving trend smoothing algorithm (based on linear approximates) is of low efficiency, when applied to series prediction. Much better smoothing and prediction properties may be reached by employing the 3.th order polynomial (s3) including only a constant and 3.th order monomial (only  $b_0$ ,  $b_3$  are to be tuned by LS method). The approximation window width  $M$  may be easily adjusted by examination the Gain Plots of the moving trend based filters in frequency domain. The recommended filter s3 enables for very effective separation of the series onto low frequency ( $\omega < \omega_r$ ) and high frequency ( $\omega \geq \omega_r$ ) components, by taking the approximation window width  $M = 1.38 * T$ .

Smoothing (reconstruction of low frequency components) is the most effective (with no delay) in the central segment of the series. In the final section the low frequency signal distortion is significant, mainly due to varying delay of the consecutive final segment filters, which decreases prediction quality. The distortion produced by the recommended filter s3 is much weaker than that of the classical moving trend smoothing.

The periodic component  $C(t)$  may be extracted from the filtering residuals by a regression method applied to residuals in the central section of the processed series.

### REFERENCES

- [1] M. Cieślak (red.), *Prognozowanie gospodarcze. Metody i zastosowanie*, PWN Warszawa, 2002
- [2] G.E.P. Box, G.M. Jenkins, G.C. Reinsel, *Time Series Analysis, Forecasting and Control*. 3rd ed. Prentice Hall, Englewood Cliffs, NJ, 1994
- [3] M.V. Askom, S. Chenouri, A.K. Mahmoodabadi: *ARCH and GARCH models*. Department of Statistics & Actuarial Sciences, University of Waterloo, 2001
- [4] R.K. Otnes, L. Enochson, *Digital Time Series Analysis*, New York: John Wiley, 1972
- [5] J.T. Duda, T. Pelech-Pilichowski, A. Augustynek, *Wykorzystanie trendu pelzającego do analizy i prognozowania szeregów finansowych*. [W:] Współczesne problemy zarządzania przedsiębiorstwami w gospodarce rynkowej (red. H. Howaniec, W. Waszkielewicz), Wyd. ATH, Bielsko-Biała, 2013 (in print)
- [6] J.T. Duda, T. Pelech-Pilichowski., *Opracowywanie prognoz sytuacji hydrogeologicznej i ostrzeżeń przed niebezpiecznymi zjawiskami zachodzącymi w strefach zasilania lub poboru wód podziemnych*. Research Report, AGH UST, Faculty of Management, Kraków, 2012